Supporting Information

Understanding the Formation of Deep Eutectic Solvents: Betaine as a Universal Hydrogen Bond Acceptor

Dinis O. Abranches,[a] Liliana P. Silva,[a] Mónia A. R. Martins,[a] Simão P. Pinho[b] and João A. P. Coutinho*,[a]

[a] CICECO – Aveiro Institute of Materials, Department of Chemistry, University of Aveiro, 3810-193 Aveiro, Portugal

[b] Centro de Investigação de Montanha (CIMO), Instituto Politécnico de Bragança. Campus de Santa Apolónia, 5300-253 Bragança, Portugal

* Corresponding author e-mail address: jcoutinho@ua.pt (João A. P. Coutinho)

Number of Pages: 22
Number of Tables: 7
Number of Figures: 11

Contents

S1. Experimental & Computational Details

Table S1. *Substances experimentally used in this work along with their CAS number, supplier, purity and water content.*

Substance	CAS Number	Supplier	Purity	Water Content (ppm)
Trimethylglycine	107-43-7	Acros Organics	98%	425[a)]
Cholinium Chloride	67-48-1	Acros Organics	98%	603[a)]
Thymol	89-83-8	TCI	>99%	22
Salicylic Acid	69-72-7	Acrofarma	99%	134
(-)-Menthol	2216-51-5	Acros Organics	99.5%	79
Coumarin	91-64-5	Sigma	99%	18
R-Camphor	464-49-3	Alfa Aesar	98%	3671
Octadecan-1-ol	112-92-5	Sigma-Aldrich	99%	25
Octadecanoic Acid	57-11-4	Acros Organics	97%	21
Urea	57-13-6	Analar	99.5%	38
Sorbitol	50-70-4	Fischer	98%	23

a) after drying.

Table S2. *Melting properties (melting temperature, T_m, enthalpy of fusion, $\Delta_m h$, and entropy of fusion, $\Delta_m s$) of the compounds studied in this work, used to calculate ideal solid-liquid equilibrium and activity coefficients.*

Compound	T_m /K	$\Delta_m h$ /kJ·mol^{-1}	$\Delta_m s$ /kJ·mol^{-1}·K^{-1}	Ref.
Trimethylglycine	566	17.98	0.0318	[1]
Cholinium Chloride	597	4.3	0.0559[a)]	[2]
Thymol	323.5	19.65	0.0607	[3]
Salicylic Acid	432.5	23.05	0.0533	[4]
(-)-Menthol	315.7	12.89	0.0408	[3]
Coumarin	342.3	18.63	0.0544	[5]
R-Camphor	450.4	5.28	0.0117	[6]
Octadecan-1-ol	331.34	65.35	0.1972	[7]
Octadecanoic Acid	343.67	61.36	0.1785	[8]
Tetramethylammonium Chloride	612.87	20.49	0.0334	[8]
Tetrabutylammonium Chloride	344.0	14.69	0.0427	[9]
Urea	407.2	14.6	0.0359	[10]
Sorbitol	366.5	30.2	0.0824	[11]

a) Value obtained considering both fusion and the solid-solid transition of the compound.

S2. Supporting Results and Discussion

S2.1 Chemical Structures

The chemical structure and the σ-surface of each molecule used in this work to prepare betaine-based systems are depicted below in Figure S1. The σ-surface is a practical visual aid to understand the polarity of the molecules and their hydrogen bond donning and/or acceptance capability. Among other interesting conclusions, the σ-surface of betaine reveals a very diffuse positive charge, as expected by the methyl group shielding of its nitrogen atom.

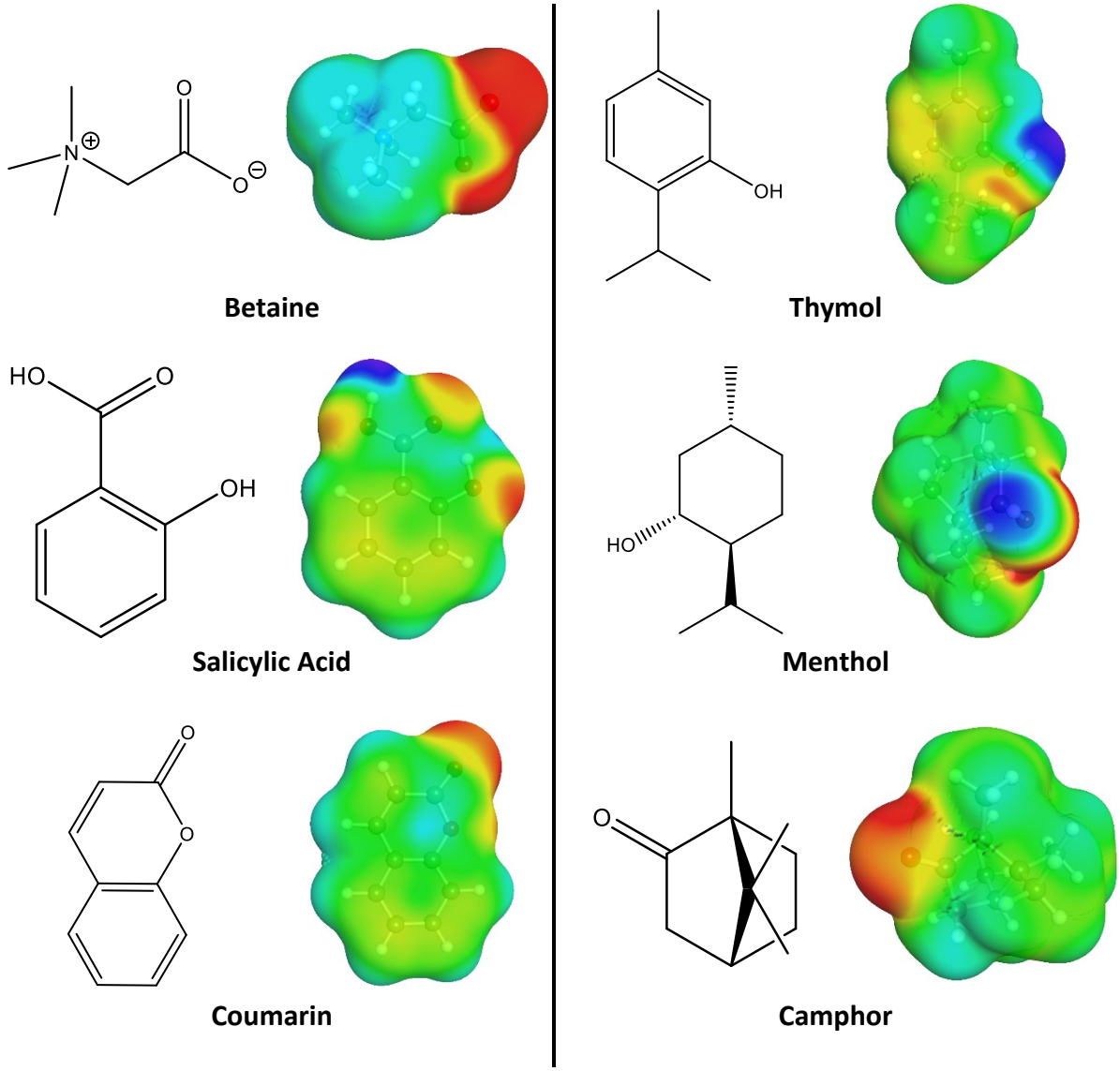

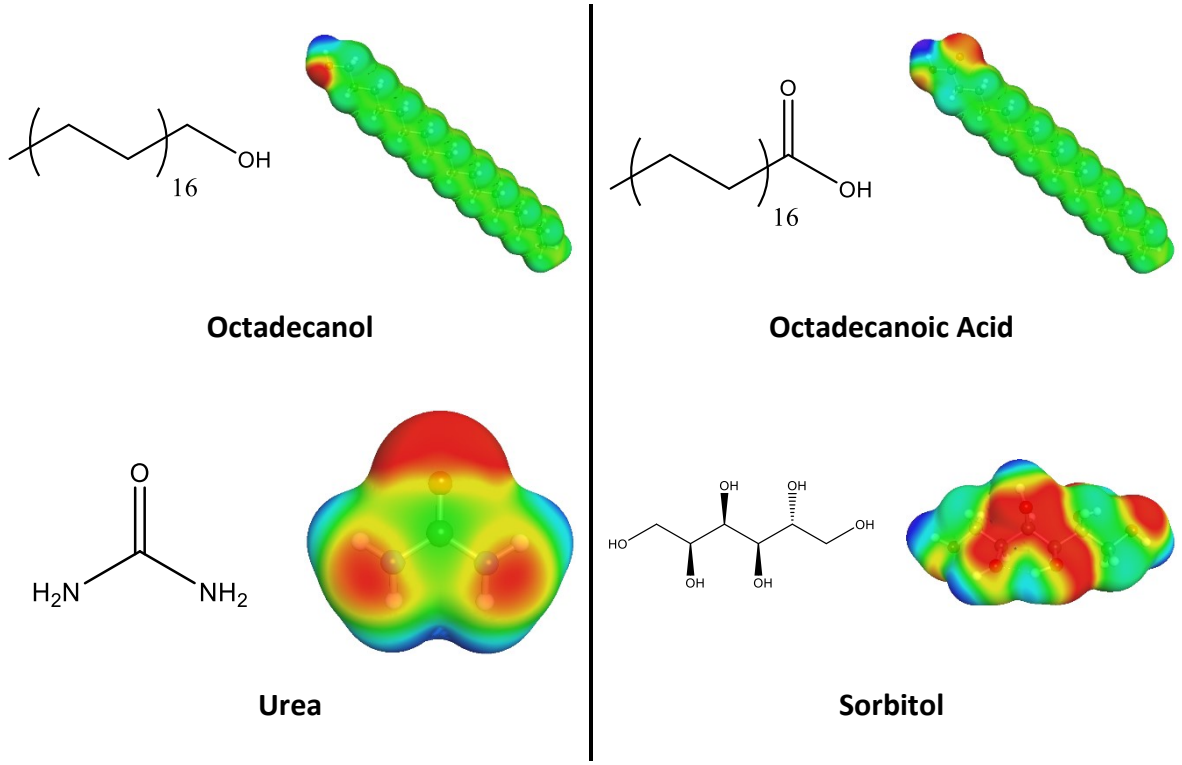

Figure S1. *Chemical structures and σ-surface of the molecules experimentally explored in this work to prepare betaine-based deep eutectic solvents.*

The chemical structures of betaine, choline and $[N_{1,1,1,1}]Cl$ are depicted below in Figure S2 to emphasize the similarity of the compounds.

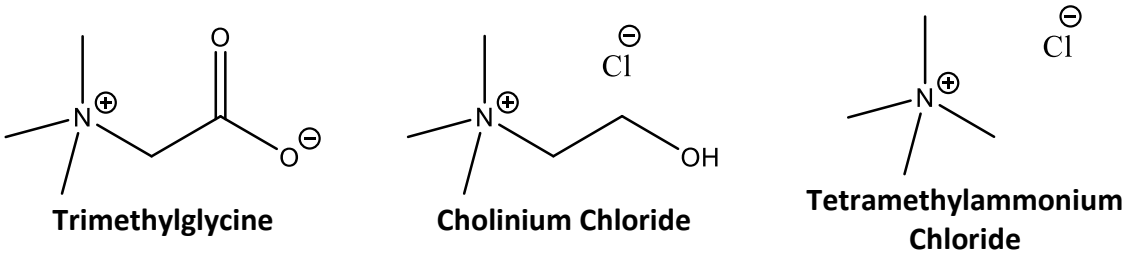

Figure S2. *Chemical structures of the quaternary ammonium-based substances compared in this work: trimethylglycine, cholinium chloride, and tetramethylammonium chloride.*

S2.2 Choline-based Systems

The solid-liquid phase diagrams of the choline-based eutectic systems measured in this work are reported below in Figure S3. Figure S4 serves to compare these solid-liquid phase diagrams with those of the betaine-based systems.

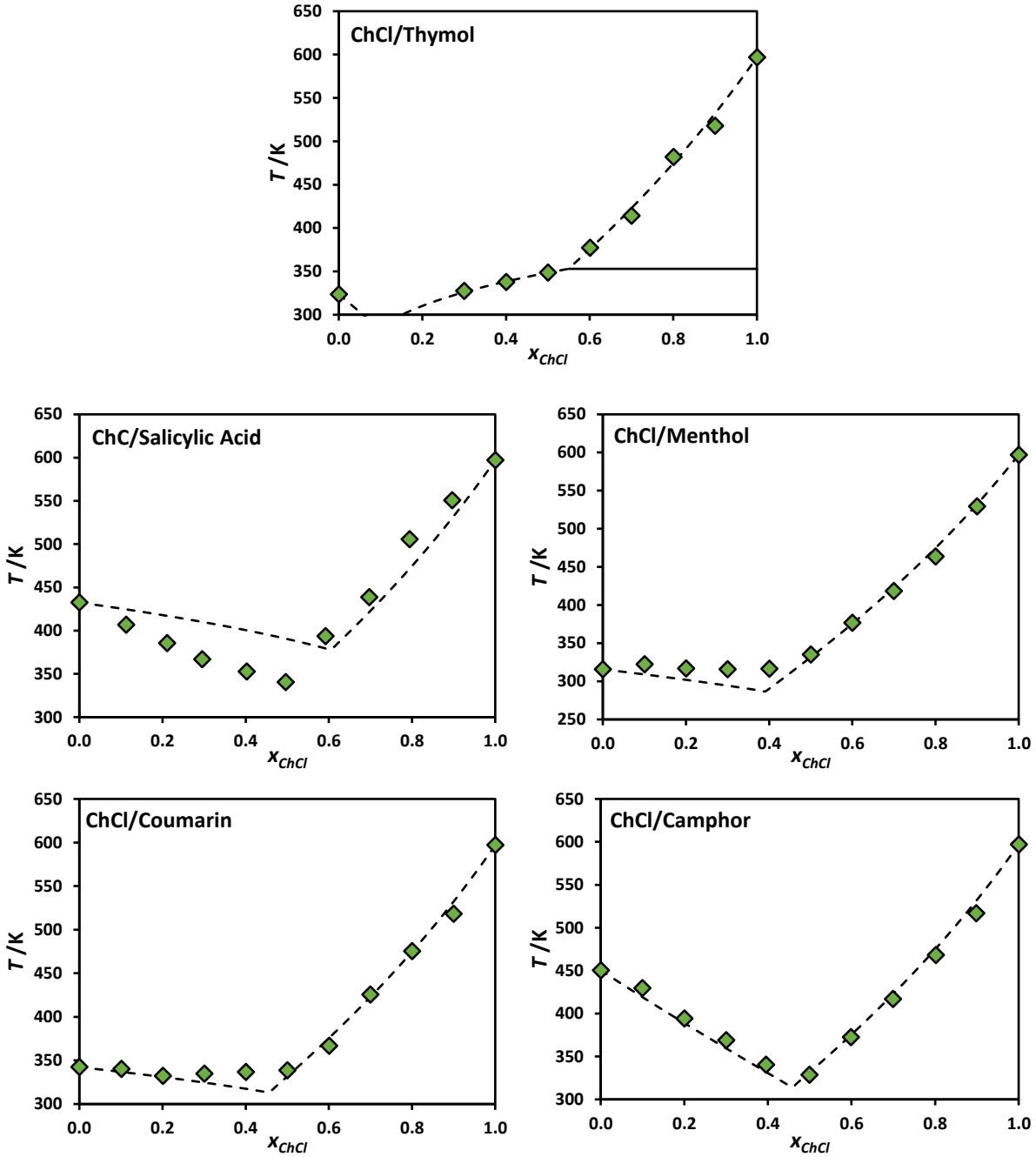

Figure S3. *Experimental solid-liquid phase diagrams (◆) of the binary systems composed of cholinium chloride (ChCl) and thymol, salicylic acid, menthol, coumarin or camphor, along with the ideal solid-liquid equilibrium phase diagram (- - -).*

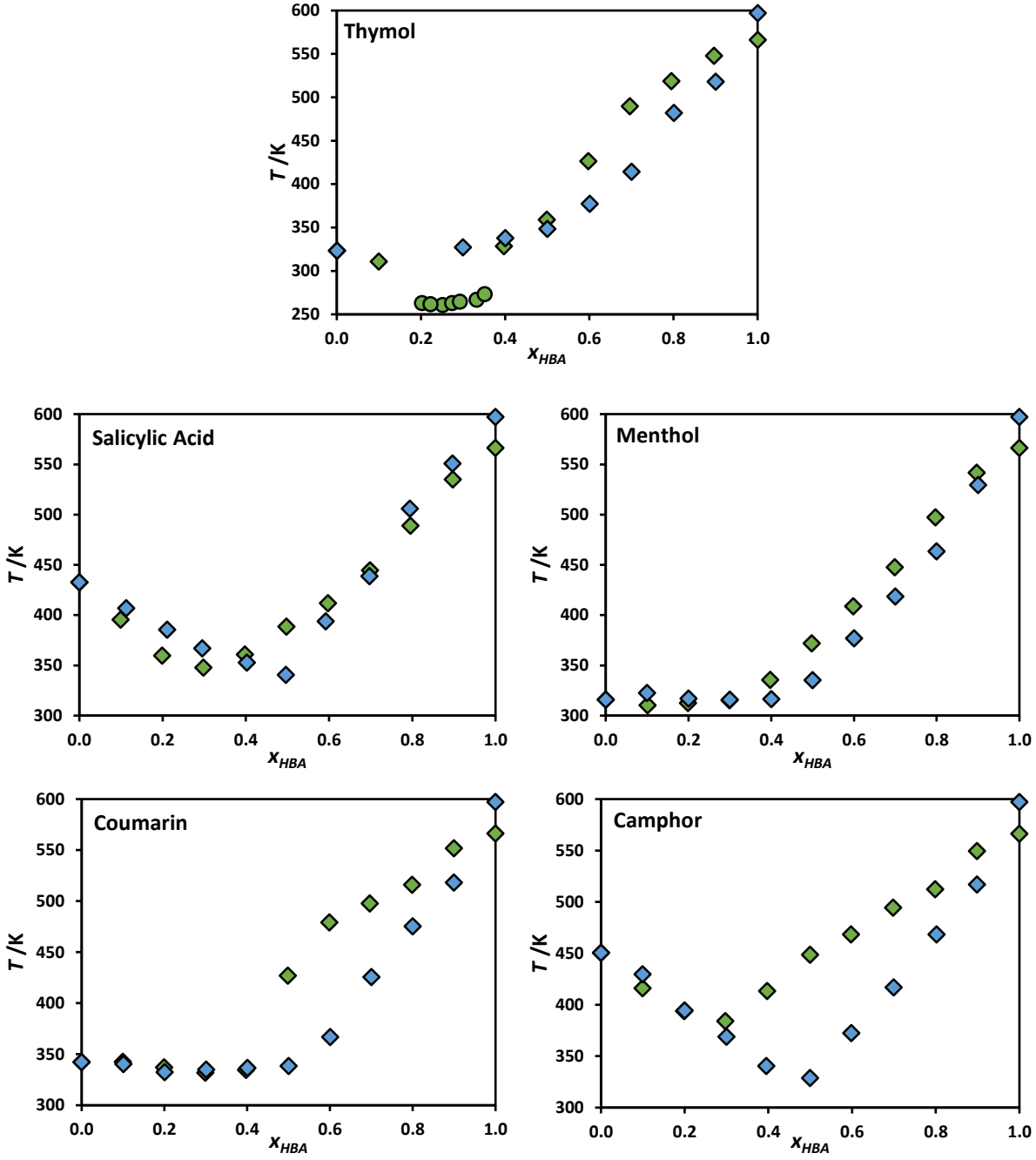

Figure S4. *Experimental solid-liquid phase diagrams of the binary systems composed of betaine (◆ this work; ● literature[12]) or choline (◆) and thymol, salicylic acid, menthol, coumarin or camphor.*

S2.3 [$N_{1,1,1,1}$]Cl Comparison

As explained in the main text, the solid-liquid phase diagrams of the systems composed of betaine and octadecanol or octadecanoic acid were measured in this work and are reported below, in Figure S5. The choice of using octadecanol and octadecanoic acid as components to probe the similarity between betaine and [$N_{1,1,1,1}$]Cl lies on the fact that these compounds are model molecules for organic alcohols and carboxylic acids, and the fact that a recent study compares the behavior of a plethora of DES-forming substances (including [$N_{1,1,1,1}$]Cl) using them.[13]

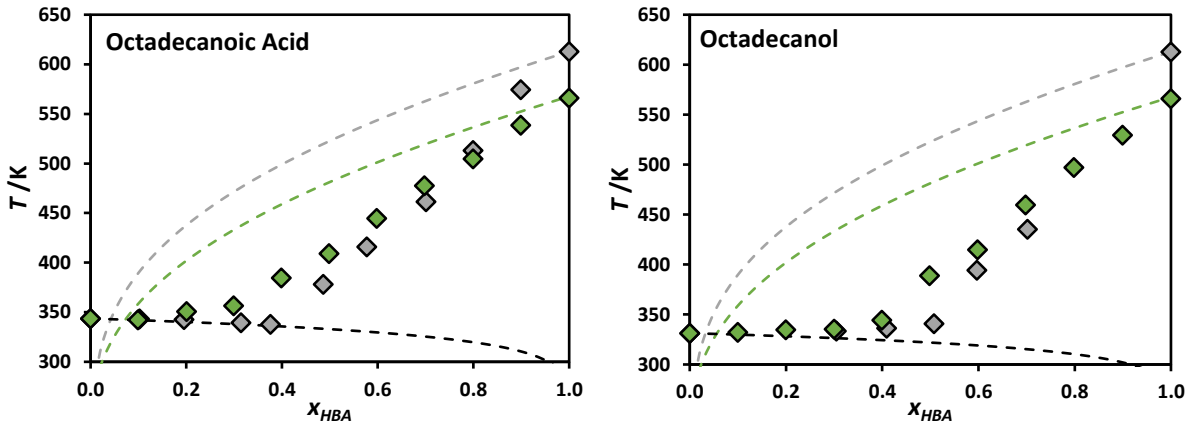

Figure S5. *Experimental solid-liquid phase diagrams of the binary systems composed of betaine (◆ this work) or tetramethylammonium chloride (◆[13]) and octadecanoic acid or octadecanol, along with the ideal liquidus line of betaine (- - -), tetramethylammonium chloride (- - -) and octadecanol or octadecanoic acid (- - -).*

S2.4 Water Impact

The impact of water in the systems betaine/menthol and betaine/sorbitol was probed in this work by measuring the solid-liquid phase diagram of these systems without water or in the presence of 2 wt% of water. These results are reported below in Figure S6.

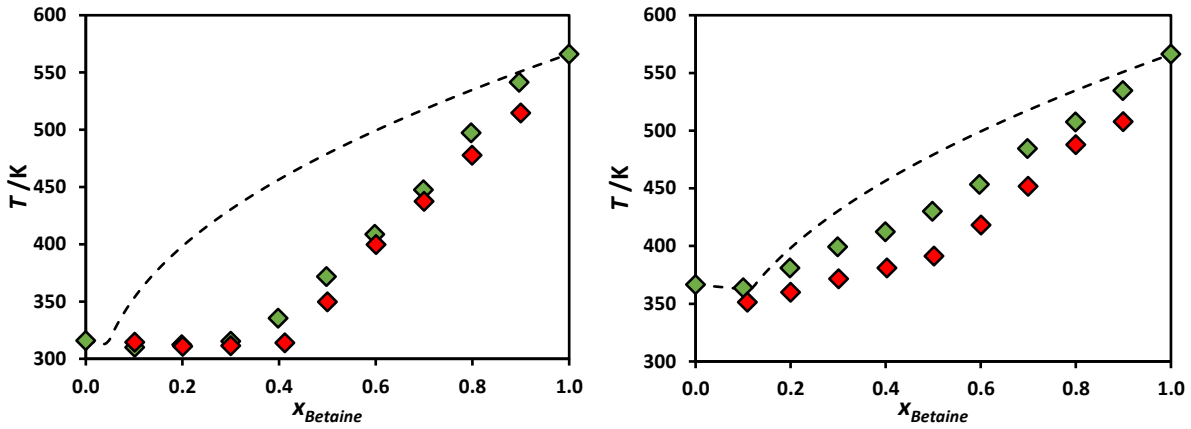

Figure S6. *Experimental solid-liquid phase diagrams of the binary systems composed of betaine and menthol (left) or sorbitol (right) without water (◇) or with 2 wt% water (◆), along with the ideal solid-liquid equilibrium phase diagram (- - -).*

S2.5 Polarity Factors

As suggested in the main text, betaine negative deviations to ideality when mixed with other substances seem to correlate with their hydrogen bond donning ability. To show this, polarity factors are here proposed based on the unnormalized σ-profile framework of COSMO-RS.[14,15] The σ-profile of a molecule is a histogram encoding the amount of molecular surface with a given polarization charge-density, σ,[16,17] which was calculated from the σ-surface of the molecules (see experimental section of the main text) using the software COSMOtherm[18] with the BP_TZVP_19.ctd parametrization.

Within the framework of the σ-profile, $p(\sigma)$, values of σ lower than -0.0082 e/Å^2 correspond to positive area segments of the molecule and values higher than 0.0082 e/Å^2 correspond to negative segments.[16,17] Thus, it is here proposed that the amount of positive (P^+) and negative (P^-) surface area of a molecule can be defined as integrals of its σ-profile in the following manner:

$$P^+ = \int_{-\infty}^{-0.0082} p(\sigma) \cdot |\sigma| \cdot d\sigma \quad \text{(S1)}$$

$$P^- = \int_{0.0082}^{+\infty} p(\sigma) \cdot \sigma \cdot d\sigma \quad \text{(S2)}$$

Note that the terms $|\sigma|$ and σ in Equations S1 and S2, respectively, weight the contribution of a given polarity area of a molecule to the final value of the polarity factor. That is, the polarity factors defined in Equations S1 and S2 do not simply sum the positive and negative areas of a molecule; instead, the more polar a particular area segment is, the more it contributes to the final value of the polarity factor. These definitions are in line with a previous work, where a similar factor was defined in order to quantify the apolarity of a molecule and successfully used to explain dissolution phenomena.[19]

The P^+ and P^- factors were calculated for each compound studied in this work with betaine using the aforementioned procedure and are reported in Table S3.

Table S3. *Polarity factors of the compounds whose mixtures with betaine were studied in this work.*

Substance	P^+ (10^3)	P^- (10^3)
Betaine	0.242	0.703
Coumarin	0.070	0.295
Menthol	0.080	0.176
Camphor	0.000	0.239
Salicylic Acid	0.180	0.233
Thymol	0.131	0.093
Urea	0.389	0.421
Octadecanol	0.103	0.195
Octadecanoic Acid	0.137	0.274
Sorbitol	0.455	0.732

As explained in the main text, for a binary system composed of betaine and a second component, the amount of positive polarity of the latter contributes favorably to betaine negative deviations to ideality while negative polarity contributes unfavorably. As such, the melting temperature of each system, taken at $x_{betaine} = 0.5$, was correlated against the difference between the polar factors of the second component ($P^+ - P^-$). These results are reported below in Figure S7.

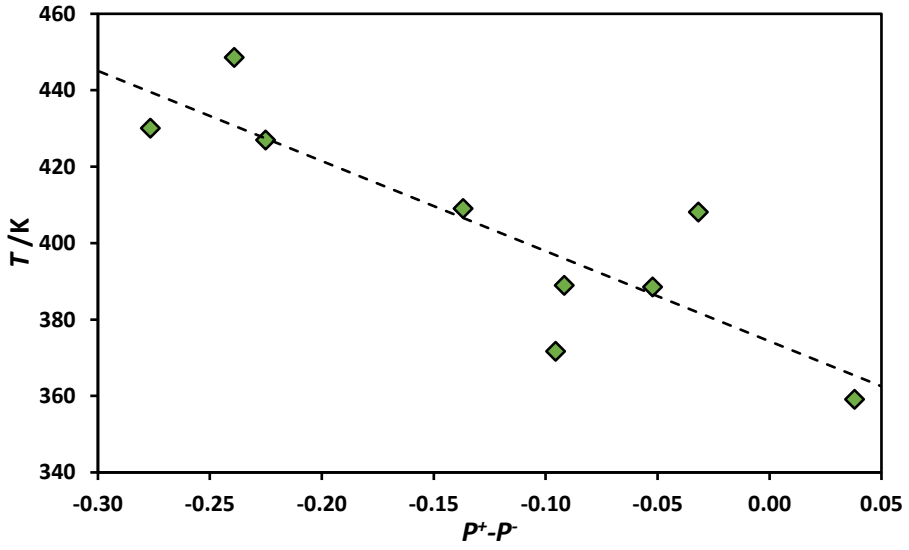

Figure S7. *Melting temperature of the betaine-based mixtures discussed in this work ($x_{Betaine}$ = 0.5) as a function of the excess positive polarity of the second component, calculated using the polar factors proposed in this work. The dashed line is the straight line obtained using the method of least squares, and the resulting coefficient of determination is 0.73.*

S2.6 Betaine-Urea-Water Interaction Energies

The most stable molecular pairs of the betaine/urea system were optimized, and their interaction energies were calculated, as described in the experimental section of the main text. These results are reported in Figure S8 and show that betaine-betaine contacts are not favorable, while betaine-urea contacts are more favorable than urea-urea contacts. Thus, Figure S8 explains the thermodynamic deviations of the betaine/urea system, since the betaine-urea interaction is stronger than betaine-betaine or urea-urea interactions.

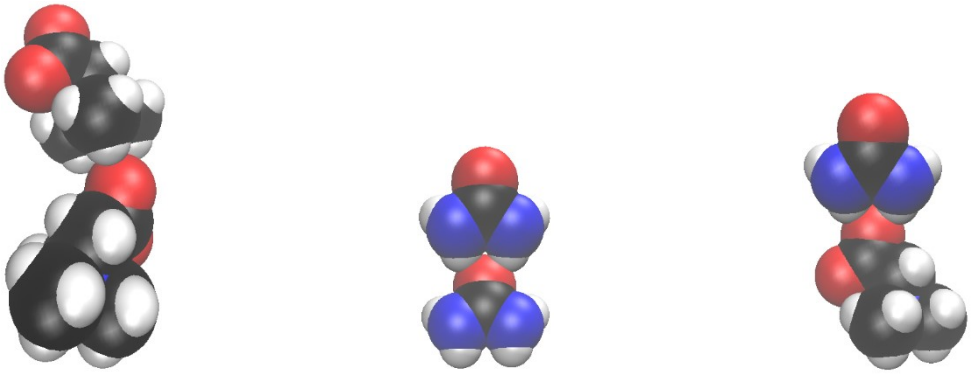

Betaine-Betaine	**Urea-Urea**	**Betaine-Urea**
4 kJ/mol	**-11 kJ/mol**	**-13 kJ/mol**

Figure S8. *Optimized structures and interaction energy of the binary pairs betaine-betaine, urea-urea and betaine-urea. Black, white, red and blue beads correspond to carbon, hydrogen, oxygen and nitrogen atoms, respectively. Representation based on the Van der Waals radius of the atoms.*

To understand the peculiar impact of water on the betaine/urea system, the most stable betaine-urea-water complex was optimized, and its interaction energy calculated, as explained in the experimental section of the main text. This result is reported in Figure S9 (left) and shows that betaine, urea and water form a very strong complex (interaction energy is approximately double the interaction energy of betaine-urea). This complex consists of a water molecule bridging a proton from the amine group of urea and an oxygen of the carboxylate group of betaine, and the carbonyl group of urea contacting the quaternary ammonium of betaine. Note that, without the water molecule, betaine and urea cannot form a good contact in a similar geometry (carbonyl group of urea interacting with the quaternary

ammonium of betaine and a proton of the amine group of urea contacting an oxygen atom of betaine), as demonstrated in Figure S9 (right).

Betaine-Urea-Water

-24 kJ/mol

Betaine-Urea

-7 kJ/mol

Figure S9. *Optimized structures and interaction energy of the most stable betaine-urea-water complex (left) and a betaine-urea contact (right) with similar geometry to the complex. Black, white, red and blue beads correspond to carbon, hydrogen, oxygen and nitrogen atoms, respectively. Representation based on the Van der Waals radius of the atoms.*

S2.7 Betaine Enthalpy of Fusion

Throughout this work, the ideal liquidus line of betaine is calculated (see experimental section of the main text) considering a value of 17.98 kJ/mol for its enthalpy of fusion. Note, however, that the direct measurement of the enthalpy of fusion of betaine is difficulted by its decomposition upon melting. Nevertheless, Wang and co-authors[1] estimated the value of 17.98 kJ/mol using a group contribution method, stating it to be consistent with their experimental DSC (differential scanning calorimetry) results, and successfully used it to describe the solubility of betaine in different solvents.

The enthalpy of fusion of a substance can be calculated from solid-liquid equilibrium data by rearranging Equation 1 of the main text, leading to:

$$\Delta_m h_i = \frac{R \cdot \ln(x_i)}{\left(\frac{1}{T_{m,i}} - \frac{1}{T}\right)} + \frac{R \cdot \ln(\gamma_i)}{\left(\frac{1}{T_{m,i}} - \frac{1}{T}\right)} \quad \text{(S3)}$$

However, the activity coefficient of the substance in the mixture needs to be known. Since this value depends on the composition of the substance and approaches unity as the substance mole fraction tends to one, a simple estimate for the enthalpy of fusion of betaine can be given by eliminating part of the right-hand-side of Equation S3, leading to:

$$\Delta_m h_i = \frac{R \cdot \ln(x_i)}{\left(\frac{1}{T_{m,i}} - \frac{1}{T}\right)}, \gamma_i = 1 \quad \text{(S4)}$$

Equation S4 was applied to the solid-liquid equilibrium data points for all mixtures measured in this work at a betaine mole fraction of 0.9. This procedure was carried out to confirm that the enthalpy of fusion of betaine estimated by Wang and co-authors[1] is not a *gross* estimate. Thus, Equation S4 was used to calculate an enthalpy of fusion of betaine using each of the nine betaine-based systems here experimentally measured (binary mixtures of betaine and thymol, menthol, coumarin, camphor, salicylic acid, octadecanol, octadecanoic acid, urea or sorbitol). The average of the values obtained for each system is 11.4 kJ/mol. Note, however, that this figure is underestimated, since the systems mentioned above present, as explained in the main text, severe negative deviations to ideality (note the second part of the right hand side of Equation S3). Still, it serves to support the value obtained by Wang and co-authors[1] and strengthens the discussion of this work based on the ideal liquids line of betaine.

S2.8 Betaine Hydrochloride

The main interactions of betaine hydrochloride (betaine HCl), a commercially available form of betaine, as a hydrogen bond acceptor should happen through its chloride anion, instead of the carboxylate group, since the carboxylate group is protonated. Furthermore, the proton of the protonated carboxylate group of betaine hydrochloride should establish a strong hydrogen bond with the chloride anion, limiting its ability to induce negative deviations to ideality in other compounds. Its behavior is thus expected to be closer to the behavior of cholinium chloride rather than betaine, with the universality of betaine as a hydrogen bond acceptor being lost in betaine hydrochloride. Note below the structures of betaine, betaine hydrochloride and cholinium chloride:

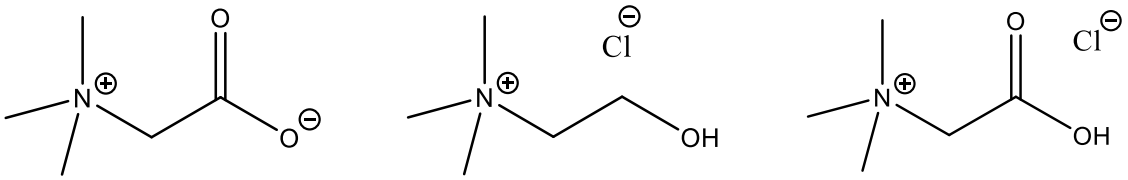

Figure S10. *Chemical structures of trimethylglycine, cholinium chloride, and betaine hydrochloride.*

The study of betaine hydrochloride is further undermined by the difficulty of measuring its enthalpy of fusion, which is not available in the literature, due to decomposition upon melting, similar to what happens with betaine and cholinium chloride. The solid-liquid phase diagram of the system betaine HCl/thymol was measured in this work and is reported below in Figure S11.

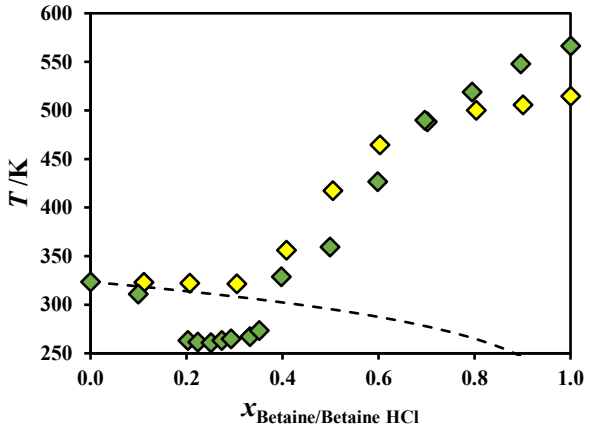

Figure S11. *Experimental solid-liquid phase diagrams of the binary system composed of thymol and betaine (◆) or betaine hydrochloride (◇), along with the ideal solid-liquid equilibrium curve of thymol (- - -).*

Figure S11 shows that betaine HCl is unable to induce negative deviations to ideality on thymol, contrary to betaine, as expected. Considering that thymol is the strongest hydrogen bond donor studied in this work, betaine HCl is expected to also be unable to induce negative deviations to ideality in the remaining compounds studied. No conclusion can be drawn about the deviations to ideality of betaine HCl itself due to the unavailability of its enthalpy of fusion.

S3. Experimental Data

Table S4. *Experimental solid-liquid equilibrium data (mole fraction, x, melting temperature, T, and activity coefficient, ϒ) measured in this work at atmospheric pressure for binary betaine-based systems.*

x_1	T /K	Υ_1	x_1	T /K	Υ_2
Betaine (1) + Thymol (2)					
0.896	547.9	0.982	0.099	310.9	0.826
0.795	518.8	0.887			
0.696	489.7	0.791			
0.598	426.4	0.478			
0.499	359.2	0.222			
0.397	328.5	0.159			
Betaine (1) + Menthol (2)					
0.897	541.5	0.937	0.299	315.2	1.416
0.797	497.3	0.739	0.199	312.3	1.184
0.698	447.5	0.520	0.101	310.1	1.018
0.598	408.6	0.383			
0.498	371.7	0.272			
Betaine (1) + Coumarin (2)					
0.899	551.7	1.006	0.299	331.9	1.162
0.798	516.0	0.864	0.199	336.9	1.123
0.696	497.5	0.848	0.099	342.4	1.112
0.598	479.2	0.835			
0.498	427.0	0.578			
0.397	334.6	0.179			
Betaine (1) + Camphor (2)					
0.898	549.5	0.991	0.198	393.8	1.019
0.799	512.2	0.837	0.099	415.9	0.988
0.698	494.3	0.822			
0.598	468.4	0.754			
0.499	448.6	0.736			
0.397	413.4	0.614			
0.297	384.0	0.549			
Betaine (1) + Salicylic Acid (2)					
0.897	534.8	0.891	0.298	347.8	0.299
0.796	488.8	0.687	0.199	359.7	0.341
0.698	444.6	0.504	0.099	395.4	0.608
0.597	411.8	0.400			
0.497	388.5	0.351			

0.398	360.8	0.286			
Betaine (1) + Octadecanol (2)					
0.899	529.6	0.854	0.300	335.4	1.898
0.798	497.3	0.738	0.200	334.8	1.595
0.698	459.7	0.592	0.100	332.1	1.172
0.598	415.0	0.416			
0.498	389.0	0.352			
0.399	344.2	0.214			
Betaine (1) + Octadecanoic Acid (2)					
0.899	538.5	0.914	0.099	342.2	1.011
0.799	504.7	0.786			
0.698	477.7	0.706			
0.598	444.5	0.588			
0.498	409.0	0.463			
0.398	384.6	0.413			
0.299	356.7	0.355			
0.200	350.6	0.477			
Betaine (1) + Urea (2)					
0.901	522.2	0.805	0.192	359.3	0.697
0.793	490.4	0.699	0.100	390.7	0.926
0.688	458.2	0.591			
0.615	435.5	0.517			
0.497	408.1	0.459			
0.380	386.3	0.444			
0.299	369.5	0.438			
Betaine (1) + Sorbitol (2)					
0.899	534.7	0.888	0.100	363.9	1.034
0.799	507.4	0.804			
0.698	484.6	0.753			
0.597	453.3	0.647			
0.498	430.1	0.600			
0.399	412.4	0.603			
0.299	399.3	0.678			
0.198	381.0	0.788			

Estimated uncertainty of T is lower than 1 K.

Table S5. *Experimental solid-liquid equilibrium data (mole fraction, x, melting temperature, T, and activity coefficient, ϒ) measured in this work at atmospheric pressure for binary choline-based systems.*

x_1	T /K	Υ_1	x_1	T /K	Υ_2
ChCl (1) + Thymol (2)					
0.900	518.0	0.974			
0.801	482.0	1.016			
0.700	414.2	0.975			
0.601	377.2	1.005			
0.500	348.6	1.002			
0.400	337.9	0.992			
0.300	327.4	1.034			
ChCl (1) + Menthol (2)					
0.900	529.3	0.994	0.400	316.3	1.682
0.800	463.4	0.974	0.300	315.7	1.430
0.700	418.5	0.987	0.200	316.9	1.274
0.600	376.8	1.005	0.100	322.4	1.230
0.500	335.1	1.016			
ChCl (1) + Coumarin (2)					
0.899	518.1	0.974	0.401	336.6	1.492
0.800	475.3	1.002	0.301	334.7	1.233
0.700	425.6	1.008	0.200	332.3	1.027
0.600	366.7	0.967	0.101	340.4	1.071
0.500	338.5	1.031			
ChCl (1) + Camphor (2)					
0.898	516.9	0.973	0.395	340.4	1.049
0.802	468.3	0.983	0.300	368.9	1.046
0.699	416.7	0.983	0.200	394.2	1.023
0.599	372.3	0.990	0.100	429.6	1.037
0.499	328.7	0.987			
ChCl (1) + Salicylic Acid (2)					
0.896	550.7	1.037	0.403	352.7	0.392
0.794	505.7	1.077	0.295	366.8	0.450
0.697	438.7	1.049	0.211	385.4	0.579
0.592	393.6	1.080	0.113	406.9	0.752
0.496	340.6	1.050			

Estimated uncertainty of T is lower than 1 K.

Table S6. *Experimental solid-liquid equilibrium data (mole fraction, x, melting temperature, T, and activity coefficient, ϒ) measured in this work at atmospheric pressure for betaine-based systems with 2 wt% of water.*

x_1	T /K	Υ_1	x_1	T /K	Υ_2
Betaine (1) + Urea (2) + 2 wt% Water					
0.898	502.6	0.687	0.200	344.5	0.427
0.798	463.5	0.537	0.100	367.0	0.693
0.697	426.5	0.411			
0.600	397.8	0.331			
0.501	353.9	0.202			
Betaine (1) + Menthol (2) + 2 wt% Water					
0.900	514.7	0.758	0.300	311.4	1.334
0.799	477.6	0.616	0.200	310.9	1.159
0.700	437.5	0.465	0.101	314.4	1.090
0.600	399.8	0.340			
0.500	349.7	0.188			
0.411	313.9	0.113			
Betaine (1) + Sorbitol (2) + 2 wt% Water					
0.900	507.9	0.717	0.109	351.4	0.733
0.800	487.9	0.677			
0.700	451.7	0.543			
0.601	418.1	0.430			
0.501	391.3	0.362			
0.403	380.9	0.388			
0.301	371.7	0.451			
0.200	359.9	0.560			

Estimated uncertainty of T is lower than 1 K.

Table S7. *Experimental solid-liquid equilibrium data (mole fraction, x, melting temperature, T, and activity coefficient, ϒ) measured in this work at atmospheric pressure for binary betaine hydrochloride systems.*

x_1	T /K	Υ_1	x_1	T /K	Υ_2
Betaine HCl (1) + Thymol (2)					
1	514.4	1	0.305	321.6	1.376
0.901	505.7		0.207	322.1	1.220
0.804	500.1		0.112	322.7	1.106
0.702	488.2				
0.602	464.3				
0.505	417.2				
0.408	356.2				

Estimated uncertainty of T is lower than 1 K.

S4. References

[1] S. Wang, Y. Zhang, J. Wang, *J. Chem. Eng. Data* **2014**, *59*, 2511–2516.

[2] L. Fernandez, L. P. Silva, M. A. R. Martins, O. Ferreira, J. Ortega, S. P. Pinho, J. A. P. Coutinho, *Fluid Phase Equilib.* **2017**, *448*, 9–14.

[3] M. A. R. Martins, E. A. Crespo, P. V. A. Pontes, L. P. Silva, M. Bülow, G. J. Maximo, E. A. C. Batista, C. Held, S. P. Pinho, J. A. P. Coutinho, *ACS Sustain. Chem. Eng.* **2018**, *6*, 8836–8846.

[4] M. A. Peña, B. Escalera, A. Reíllo, A. B. Sánchez, P. Bustamante, *J. Pharm. Sci.* **2009**, *98*, 1129–1135.

[5] M. A. R. Matos, C. C. S. Sousa, M. S. Miranda, V. M. F. Morais, J. F. Liebman, *J. Phys. Chem. B* **2009**, *113*, 11216–11221.

[6] D. O. Abranches, M. A. R. Martins, L. P. Silva, N. Schaeffer, S. P. Pinho, J. A. P. Coutinho, *Chem. Commun.* **2019**, *55*, 10253–10256.

[7] F. C. de Matos, M. C. da Costa, A. J. de A. Meirelles, E. A. C. Batista, *Fluid Phase Equilib.* **2016**, *423*, 74–83.

[8] P. V. A. Pontes, E. A. Crespo, M. A. R. Martins, L. P. Silva, C. M. S. S. Neves, G. J. Maximo, M. D. Hubinger, E. A. C. Batista, S. P. Pinho, J. A. P. Coutinho, et al., *Fluid Phase Equilib.* **2017**, *448*, 69–80.

[9] D. O. Abranches, N. Schaeffer, L. P. Silva, M. A. R. Martins, S. P. Pinho, J. A. P. Coutinho, *Molecules* **2019**, *24*, 3687.

[10] U. S. Rai, R. N. Rai, *J. Mater. Res.* **1999**, *14*, 1299–1305.

[11] E. S. Domalski, E. D. Hearing, *J. Phys. Chem. Ref. Data* **1996**, *25*, 1–525.

[12] M. Tiecco, F. Cappellini, F. Nicoletti, T. Del Giacco, R. Germani, P. Di Profio, *J. Mol. Liq.* **2019**, *281*, 423–430.

[13] D. O. Abranches, R. O. Martins, L. P. Silva, M. A. R. Martins, S. P. Pinho, J. A. P. Coutinho, *J. Phys. Chem. B* **2020**, acs.jpcb.0c02386.

[14] A. Klamt, V. Jonas, T. Bürger, J. C. W. Lohrenz, *J. Phys. Chem. A* **1998**, *102*, 5074–5085.

[15] A. Klamt, *J. Phys. Chem.* **1995**, *99*, 2224–2235.

[16] J. Palomar, J. S. Torrecilla, J. Lemus, V. R. Ferro, F. Rodríguez, *Phys. Chem. Chem. Phys.* **2010**, *12*, 1991.

[17] A. Klamt, *COSMO-RS: From Quantum Chemistry to Fluid Phase Thermodynamics and Drug Design*, Elsevier Science, **2005**.

[18] COSMOtherm, Release 19; COSMOlogic GmbH & Co. KG, http://www.cosmologic.de.

[19] D. O. Abranches, J. Benfica, B. P. Soares, A. Leal-Duaso, T. E. Sintra, E. Pires, S. P. Pinho, S. Shimizu, J. A. P. Coutinho, *Chem. Commun.* **2020**, *56*, 7143–7146.